Supplemental Methods

Linkage analysis

A linkage analysis for Kindred A has been published elsewhere (15). For Kindred B, we extracted genomic DNA from cell lines or blood samples from patient P2.1 and both parents. For these individuals, we genotyped the microsatellites from D8S1722 to D8S1833 (17 microsatellites in and around the previously reported region). Multipoint Lod scores were calculated with MERLIN software (http://www.sph.umich.edu/csg/abecasis/merlin/index.html), assuming that the gene responsible for the defect was autosomal recessive and displayed full penetrance.

Cell purification and culture

Fresh human peripheral blood mononuclear cells (PBMCs) were isolated by Ficoll-Hypaque density gradient centrifugation (Amersham Pharmacia Biotech, Sweden) from heparin-treated whole-blood samples obtained from patients or healthy volunteers.

EBV-B cells were obtained by immortalizing PBMCs with Epstein-Barr virus and culturing them in complete RPMI 1640 medium (Gibco BRL, Invitrogen, USA) supplemented with 10% heat-inactivated fetal calf serum (FCS) (Gibco BRL, Invitrogen, USA).

Primary human fibroblasts were obtained from skin biopsy specimens from patients or healthy controls and were cultured in DMEM (Gibco BRL, Invitrogen, USA) supplemented with 10% fetal calf serum (FCS) (Gibco BRL, Invitrogen, USA). They were then transformed with SV40-large T antigen vector, to obtain immortalized SV40-fibroblast cell lines.

Polymorphonuclear leukocytes (PMNs) were prepared from heparin-treated blood from patients and healthy controls. Peripheral blood was subjected to dextran sedimentation

and the buffy coat was centrifuged through Ficoll-Hypaque (Amersham Pharmacia Biotech, Sweden). The remaining red blood cells were removed by hypotonic shock.

B cells, monocytes, T cells and NK cells were isolated from peripheral PBMCs by positive immunomagnetic depletion, with antibodies against CD19, CD14, CD3 and CD56 (Macs; Miltenyi Biotec, Germany), respectively, according to the kit manufacturer's instructions. The preparations of B cells, monocytes, T cells and NK cells were >90%, >80%, >70% and >90% pure, respectively (flow cytometry, not shown).

Monocyte-derived dendritic cells (MDDCs) were obtained from purified monocytes cultured in the presence of GM-CSF (50 ng/ml; R&D Systems, USA) and IL-4 (10 ng/ml; R&D Systems, USA). We plated 2 x 10^6 monocytes in complete RPMI 1640 medium (RPMI medium supplemented with 10% heat-inactivated pooled FBS (Gibco BRL, Invitrogen, USA)) in 20 cm^2 flasks and incubated them at 37°C under an atmosphere containing 5% CO_2; the medium was replaced every two days during the 10-day culture period.

Monocyte-derived macrophage cells (MDMs) were obtained from purified monocytes cultured in the presence of M-CSF (50 ng/ml; R&D Systems, USA). We plated 2 x 10^6 monocytes in complete RPMI 1640 medium (RPMI medium supplemented with 10% heat-inactivated pooled FCS), in 100 x 20 mm tissue culture dishes, and incubated them at 37°C under an atmosphere containing 5% CO_2; the medium was replaced every 5 days during the 15-day culture period.

DNA, RNA, PCR, sequencing and sequence alignment

Genomic DNA was purified from EBV-B cells or SV40 fibroblasts, by phenol/chloroform extraction. Total RNA was extracted from EBV-B cells from P1.2 and controls, and from SV40-fibroblasts of P2.1 and controls, with Trizol (Invitrogen, USA). The RNA was reverse-transcribed with SuperScript™ II Reverse Transcriptase (Invitrogen, USA),

according to the manufacturer's instructions. *MCM4* cDNA was amplified with two pairs of primers: Pair 1 (-183Forward: CCAGGTGGACTCGGAGTCC/+1560Reverse: CGAGGTTGTACACGTACTGC) and Pair 2 (+1380Forward: GAGGCTTGCTTCAGCCTTGG/+3228Reverse: CCATAAGCATACTGATGATGGC). The sequences of the primers used for the PCR amplification of exons and cDNA for all genes in the candidate region are available upon request. PCR was performed with *Taq* polymerase (Invitrogen, USA). The products were sequenced with the Big Dye Terminator cycle sequencing kit and analyzed on a 3130 ABI Prism Genetic Analyzer (Applied Biosystems, USA). The MCM4 sequences from *Ensembl* were aligned, with the CLUSTALW2 multiple sequence alignment tool.

Determination of mRNA levels by quantitative real-time RT-PCR

Total RNA was extracted from cells with Trizol reagent (Invitrogen, USA). Each RNA preparation was reverse transcribed directly with the High Capacity RNA-to-cDNA kit (Applied Biosystems, USA), after purification with the RNeasy plus Micro Kit (Qiagen, Germany) according to the manufacturer's instructions, to determine *MCM4* transcript levels (Hs00381539_m1, Applied Biosystems, USA). Quantitative real-time PCR (qPCR) was performed in an ABI PRISM® 7700 Sequence Detection System (Applied Biosystems, USA). The PCR program was as follows: 95°C for 20 seconds and then 40 cycles of 95°C for 3 seconds and 60°C for 1 minute. The results were normalized with respect to values for transcripts of the housekeeping gene encoding β-glucuronidase (GUS). Results are expressed according to the ΔCt method, as described by the kit manufacturer.

siRNA transfection

SV40-fibroblasts from P2.1 and healthy controls were transfected with 3 different siRNAs (si793 (GCAUUGAAGACUAAGAAUA), si1299 (UGAAGAAGCAGAACAGAAA) and si1325 (CAGAGAAACGUGUGGAAUU)) directed against MCM4 (from Dharmacon), and negative control siRNAs directed against luciferase (GL3) and Epstein-Barr virus nuclear antigen (EBNA) (from Dharmacon). Cells were lysed and analyzed 48 hours after transfection.

Supplemental Table legends

Supplemental Table 1 Details of the intra- and extrauterine growth retardation and adrenal insufficiency phenotypes of patients. Full-face and profile images of P1.1, P1.2 and P1.3 are shown.

Supplemental Table 2 Detailed chromosomal aberrations of primary and SV40-fibroblast cells in P1.3 and P2.1. Comparison with controls, in the presence or absence of APH treatment. Detailed descriptions of the chromosomal aberrations in cells transduced with lentiviral particles containing empty, WT *MCM4* or mutated *MCM4* allele vectors.

Supplemental Table 3 Detailed chromosomal aberrations in lymphocytes. Chromosomal aberrations, with the number of normal cells, and numbers of gaps, breaks and exchanges in total cells and in control cells included in the same experiment, after treatment with DEB, MMC and HN2.

Supplemental Figure legends

Supplemental Figure 1 (**A**) Table of all variants (other than the causal *MCM4* variant) identified in the coding region, splicing site and the 5' and 3'UTRs of all coding genes and one miRNA located in the centromeric region of chromosome 8. (**B**) Amplification of the *MCM4* cDNA as two fragments. Schematic diagram of the *MCM4* cDNA, showing the binding sites of the primers and the size of the amplification products. Amplification of the *MCM4* cDNA from SV40 fibroblatsts with various primer pairs for controls and patients. (**C**) Relative quantification of *MCM4* mRNA in EBV-B cells from P1.2, family members (n=7, 2 WT/WT, 5 WT/c.71-2A>G) and controls (n=2) and SV40-fibroblasts and primary fibroblasts from P1.3, P2.1 and controls (n=2). We used only probes specific for *MCM4* mRNA. GUS was used as endogenous gene for comparison. The ratio of *MCM4* to GUS mRNA levels is shown. Error bars indicate the standard deviation. (**D**) MCM4 was detected with a polyclonal antibody, at a size of 100 kDa, in total extracts of EBV-B cells from P1.2, WT/WT family members (n=2), WT/c.71-2A>G family members (n=6) and controls (n=2). An antibody against GAPDH was used as a protein loading control.

Supplemental Figure 2 (**A**) MCM4 protein production in SV40-fibroblasts from controls, P1.3 and P2.1 was assessed by western blotting with a polyclonal antibody against either the N-terminal domain or the C-terminal domain of MCM4 and a polyclonal antibody against the first 300 amino acids of the MCM4 protein. β-actin antibody was used as a protein loading control. (**B**) MCM4 protein levels after transient transfection with 3 different siRNAs against MCM4 in primary and SV40-fibroblasts from controls and P1.3 assessed by western blotting. Transient transfection with the control siRNAs (EBNA and GL3) was used as a negative control. Total protein extracts from controls and P1.3 primary and SV40-fibroblasts were used

as a positive control for the antibody. α-Tubulin antibody was used as a loading control. (**C**) Cell cycle of SV40-fibroblasts from controls and patients after treatment with 0.3 μM Aph. Representative flow cytometry plots. Control (left), P1.3 (middle) and P2.1 (right) after Aph treatment. P1 corresponds to normal G1 phase, P2+P3+P4 correspond to normal S phase, P5 corresponds to normal G2 phase plus abormal G1 or failed mitosis, P6+P7 correspond to re-replication S phase and P8 corresponds to 8C DNA content. The patients' SV40-fibroblasts had a lower proportion of BrdU-positive cells at S phase than the control cells (**D**) Representative spreads of chromosome breaks induced in the presence or absence of APH. A P2.1 metaphase with some aberrations indicated by arrows (left) and a P2.1 metaphase with aphidicolin-induced breaks indicated by arrows (right). The number of chromosome breaks (mean) per metaphase in P1.3 and P2.1 primary fibroblasts was not significantly different from that in control primary fibroblasts. Error bars indicate SEM.

Supplemental Figure 3 The N-terminal domain of the MCM4 protein in humans and the corresponding region in 45 other eukaryotic species. Conservation of the first 83 amino acids of the MCM4 protein, with the position of the three ATG codons in frame.

Supplemental Figure 4 Hematopoietic cell phenotypes in humans and mice (**A**) Flow cytometry for lymphocyte subsets: B cells, T cells (CD3+, CD3+CD4+,CD3+CD8+) and NK cells were detected in the peripheral blood of controls and patients (P1.1, P1.2, P1.3 P1.4, P1.5 and P2.1). Horizontal bars represent medians. (**B**) Flow cytometry for monocyte subsets: CD14+, CD16+, CD14/16+ and PDCsBDCA2+ and MDCsBDCA1+ cells were detected in the peripheral blood of controls of various age groups (5 to 10 y, 10 to 15 y and >15 y), heterozygous subjects and homozygous patients (P1.1, P1.2 and P1.3). Error bars for the controls indicate the standard deviation. (**C**) MCM4 was detected with a polyclonal antibody,

at a size of 100 kDa, in cell subsets from blood (PBLs, PMNs, T cells, B cells, NK cells, monocytes, MDDCs and macrophages), EBV-B cells, primary and SV40 fibroblast cells from a control individual. An antibody against α-tubulin was used as a loading control. This result is representative of 3 independent experiments). (**D**) NK cell percentage in WT/WT, *Chaos3*/WT, *Chaos3*/*Chaos3* mice. The percentage of NK cells is significantly lower in *Chaos3*/*Chaos3* (n=11) than in WT/WT (n=25) mice (P <0.05 indicated by *, non parametric Wilcoxon test). Horizontal bars indicate the means. The percentage of B cells is significantly higher in *Chaos3*/*Chaos3* (n=11) than in WT/WT (n=25) mice (P <0.005 indicated by **, non parametric Wilcoxon test). A significant difference in the percentage of T cells was observed between WT/WT (n=19) and *Chaos3*/*Chaos3* (n=11) mice (P <0.05 indicated by *, non parametric Wilcoxon test).

Supplemental Figure 5 T-cell phenotypes and stimulation responses (**A**) Percentage of different T- and B-cell subsets in whole-blood samples from healthy siblings either homozygous WT or heterozygous, and patients. (**B**) Proliferation of PBMCs determined by thymidine incorporation from healthy homozygous WT or heterozygous siblings and patients were not stimulated (medium) or were stimulated with PHA (2.5 mg/ml) over 3 days. (**C**) Apoptosis of PHA-activated T-cell blasts from a control, P1.2 and P1.3 was assessed by determining propidium iodide staining in the presence or absence of stimulation with various doses of IL-2 or IL-15 over 3 days. (**D**) Flow cytometry counts of CD3+Perforin+ T cells for controls (n=6), heterozygous siblings (n=2) and patients (P1.1, P1.2 and P1.3). Horizontal bars indicate medians. A non significant difference (P>0.05) is indicated by “ns”.

Supplemental Figure 6 Homozygous *MCM4* mutation and specific NK CD56dim deficiency. (**A**) Flow cytometry counts of CD56+ NK cells that were also CD16+, for controls (n=17), heterozygous siblings (n=2) and patients (P1.1, P1.2 and P1.3), Perforin+ for controls (n=6), heterozygous siblings (n=2) and patients (P1.1, P1.2 and P1.3) and CD57+ for controls (n=8) and patient P1.3. Horizontal bars indicate medians. A significant P <0.05 is indicated by *, a P <0.005 is indicated by ** and a P <0.0005 by ***, in Student's *t*-test. (**B**) MCM4 was detected with a polyclonal antibody, at a size of 100 kDa, in nuclear extract from the CD56bright and CD56dim NK cell subsets of control blood. An antibody against β-actin was used as a protein loading control. The ratio of MCM4 to β-actin protein levels is shown for 3 independent controls from independent experiments. Error bars indicate the standard deviation. (**C**) Flow cytometry counts of the two subsets of CD56 NK cells expressing CD94 in controls (n=11), heterozygous siblings (n=2) and patients (P1.1, P1.2 and P1.3). Horizontal bars indicate medians. P <0.05 is indicated by *, a P <0.005 is indicated by ** and a non significant difference (P>0.05) by "ns". Representative flow cytometry plots of a homozygous WT sibling, a heterozygous sibling and one patient. (**D**) PBMCs from healthy controls (n=6) and from one patient (P1.3) tested in two independent experiments were stained with CFSE and stimulated for 72 h with various doses of IL-15. Apoptosis was assessed on NK subsets, by 7AAD staining. Error bars indicate the standard deviation.

Patients	Delivery Date (weeks)	Delivery type (v=vaginal, CS=Cesarean section)	Sex (F=Female, M=Male)	Intrauterine Growth Retardation			Extrauterine Growth Retardation			Developmental delay	Adrenal insufficiency		
				Birth Weight (kg, percentile)	Birth Height (cm, percentile)	Birth Head Circumference (cm,percentile)	Weight (kg, percentile)	Height (cm, percentile)	Head circumference (cm, percentile)		9 am Cortisol (nmol/l) NR>200	ACTH at diagnosis (ng/l) 9<NR< 52	Maximum cortisol concentration with ACTH stimulation NR>550
P1.1	38 +4days	V	M	2.41 (<3rd)	46 (<3rd)	32.4 (3rd)	22.4 (3rd) at 10years	123 (<3rd) at 10 years	NA (<3rd) at 1.1years	Mild cognitive developmental delay	NA	NA	NA
P1.2	37	CS	F	1.64 (<3rd)	44 (<3rd)	33 (3rd)	31.8 (<3rd) at 17.4years	142.5 (<3rd) at 17.4years	51 (normal) at 17.4years	Normal IQ	<28	<10	<28
P1.3	34	CS	M	1.8 (<3rd)	45 (<3rd)	30.6 (<3rd)	21.8 (<3rd) at 12.7years	126.6 (<3rd) at 12.7years	49.5 (<3rd) at 12.7 years	Mild cognitive developmental delay	92	>2000	88
P1.4	38	CS	M	2.3 (<3rd)	46 (<3rd)	30.6 (3rd)	31.9 (75 centile) at 10years	111.9 (3rd) at 7.1years	NA	Mild cognitive developmental delay	244	NA	192
P1.5	40 +5days	CS	F	2.5 (<3rd)	47 (<3rd)	33.5 (3rd)	13.6 (<3rd) at 5.5years	98 (<3rd) at 5.5 years	48.5 (<3rd) at 3.8 years	Mild cognitive developmental delay	215	>1250 (323)	151
P2.1	40	CS	M	2.2 (<3rd)	44 (<3rd)	34 (normal)	34.2 (<3rd) at 17.9years	158 (<3rd) at 17.6years	NA	Mild cognitive developmental delay	30	532	32

P1.1

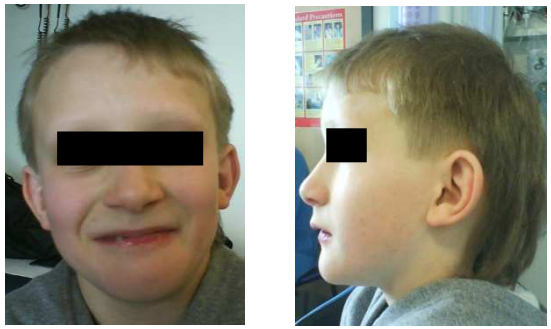

P1.2

P1.3

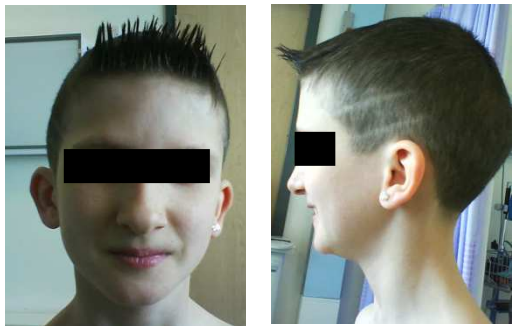

NA: Not available NR: Normal Range

Supplemental Table 1 Details of the intra- and extrauterine growth retardation and adrenal insufficiency phenotypes of patients. Full-face and profile images of P1.1, P1.2 and P1.3 are shown.

Sample	Cell Type	Drug	Concen-tration of Drug	Total Metaphases Studied	Total Breaks (ctb, rad*)	Total Chromatid Breaks (ctb*)	Total Tri-radials	Total Quadri-radials	Metaphases with Breaks	Metaphases with Multiple Breaks	Breaks per Metaphase
Control	Primary	None	-	50	0	0	0	0	0	0	0
P1.3	Primary	None	-	50	0	0	0	0	0	0	0
P2.1	Primary	None	-	26	1	1	0	0	1	0	0.04
Control	Primary	APH	0.3 μM	50	16	16	0	0	12	4	0.32
P1.3	Primary	APH	0.3 μM	57	42	36	1	2	28	9	0.74
P2.1	Primary	APH	0.3 μM	28	9	9	0	0	7	2	0.32
Control	SV40	None	-	54	0	0	0	0	0	0	0
P1.3	SV40	None	-	45	10	8	0	1	4	4	0.22
P2.1	SV40	None	-	34	6	2	1	1	3	1	0.18
Control	SV40	APH	0.3 μM	45**	37	29	1	3	16	7	0.82
P1.3	SV40	APH	0.3 μM	24***	259	233	9	4	24	22	10.79
P2.1	SV40	APH	0.3 μM	10	69	61	2	2	9	9	6.9
P1.3 + empty vector	SV40	APH	0.3 μM	20	194	172	5	6	17	14	9.7
P1.3 + MCM4wt	SV40	APH	0.3 μM	50	180	140	16	4	33	27	3.6
P1.3 + MCM4mut	SV40	APH	0.3 μM	30****	292	258	9	8	26	25	9.73

Ctb: chromatid break, rad: radial, ** 2 metaphases with significant damage (rad +ctb) were included in analysis, *** 2 metaphases with severe damage were not included in the analysis, **** 4 metaphases with severe damage were not included in the analysis.

Supplemental Table 2 Detailed chromosomal aberrations of primary and SV40-fibroblast cells in P1.3 and P2.1. Comparison with controls, in the presence or absence of APH treatment. Detailed descriptions of the chromosomal aberrations in cells transduced with lentiviral particles containing empty, WT *MCM4* or mutated *MCM4* allele vectors.

Drug[a]	Control Associated with P1.1	P1.1	Control Associated with P1.2	P1.2	Control Associated with P1.3	P1.3	Control Associated with P1.4	P1.4	Control Associated with P2.1	P2.1
DEB (0.1µg/ml)[b]	79/80 cells[c] normal 1 gap 0 break 0 exchanges	60/80 cells* normal 9 gaps 10 breaks 4 exchanges	35/40 cells normal 4 gaps 1 break 1 exchange	26/40 cells* normal 5 gaps 13 breaks 10 exchanges	ND[e]	ND[e]	39/40 cells normal 1 gap 0 break 0 exchanges	25/40 cells* normal 7 gaps 7 breaks 4 exchanges	ND[e]	ND[e]
			73/80 cells normal 5 gaps 2 breaks 0 exchanges	68/80 cells* normal 5 gaps 9 breaks 1 exchange						
MMC ($6x10^{-8}$ M)[b]	Reported abnormal[d] in clinical test for patient, in comparison with control		36/40 cells normal 3 gaps 1 break 0 exchanges	28/40 cells* normal 5 gaps 11 breaks 4 exchanges	32/40 cells normal 9 gaps 1 break 0 exchanges	30/40 cells* normal 6 gaps 7 breaks 3 exchanges	31/40 cells normal 6 gaps 2 breaks 1 exchange	22/40 cells* normal 16 gaps 6 breaks 2 exchanges	32/40 cells normal 5 gaps 1 break 2 exchanges	31/40 cells* normal 8 gaps 5 breaks 1 exchange
			23/30 cells normal 7 gaps 2 breaks 0 exchanges	22/30 cells[n] normal 6 gaps 5 breaks 2 exchanges			46/60 cells normal 10 gaps 6 breaks 3 exchanges	33/60 cells* normal 23 gaps 10 breaks 6 exchanges		
							77/100 cells normal 16 gaps 8 breaks 4 exchanges	55/100 cells* normal 39 gaps 16 breaks 8 exchanges		
HN2 (10^{-8} M)[b]	Reported abnormal[d] in clinical test for patient, in comparison with control		40/40 cells normal 0 gap 0 break 0 exchanges	27/40 cells* normal 9 gaps 8 breaks 2 exchanges	37/40 cells normal 2 gaps 1 break 0 exchanges	29/40 cells* normal 8 gaps 2 breaks 6 exchanges	NA[f]	35/40 cells* normal 2 gaps 3 breaks 0 exchanges	36/40 cells normal 1 gap 1 break 2 exchanges	26/40 cells* normal 8 gaps 5 breaks 3 exchanges
			27/30 cells normal 0 gap 4 breaks 0 exchanges	25/30 cells[n] normal 2 gaps 4 breaks 0 exchanges			NA[f]	54/60 cells* normal 2 gaps 5 breaks 0 exchanges	29/40 cells normal 9 gaps 3 breaks 0 exchanges	29/40 cells* normal 5 gaps 6 breaks 1 exchange
							NA[f]	89/100 cells* normal 4 gaps 8 breaks 0 exchanges		

[a] Drug used for DNA breakage, [b] Concentration of drug, [c] Numbers of cells normal and numbers of cells with gaps, breaks and exchanges [d,f] Details not available [e] Not done * Breakage level increases after drug treatment but not to the levels observed in Fanconi anemia patients. [n] No difference between the cells of the patient and the control

Supplemental Table 3 Detailed chromosomal aberrations in lymphocyte cells. Chromosomal aberrations, with the number of normal cells, and numbers of gaps, breaks and exchanges in total cells and in control cells included in the same experiment, after treatment with DEB, MMC and H2N.

A

Gene	Sequence analyzed	Variation	Region	Ref dbSNP database	AF[a]	Status
TACC1	cDNA	G/A	coding	rs2013586	ND	S[b]
PLEKHA2	cDNA	C/-	5'UTR	rs76319743	ND	-
ADAM9	cDNA	C/T	coding	rs61753674	0.013	S
ADAM32	gDNA	C/T	5'UTR	rs59118660	0.4547	-
IDO2	gDNA	(-/A)	3'UTR	rs78742566	0.056	-
IDO2	gDNA	A/T	3'UTR	rs33976899	ND	-
ANK1	gDNA	C/T	coding	rs1137177	0.194	S
ANK1	gDNA	C/T	coding	rs2304880	0.181	S
ANK1	gDNA	G/C	coding	rs504574	0.389	S
AP3M2	cDNA	T/A	coding	rs1050263	ND	C>S
AP3M2	cDNA	C/T	coding	rs1050264	ND	L>F
HGSNAT	cDNA	T/C	coding	rs1126058	ND	S

[a] Allele frequency [b] Synonymous ND : Not determined

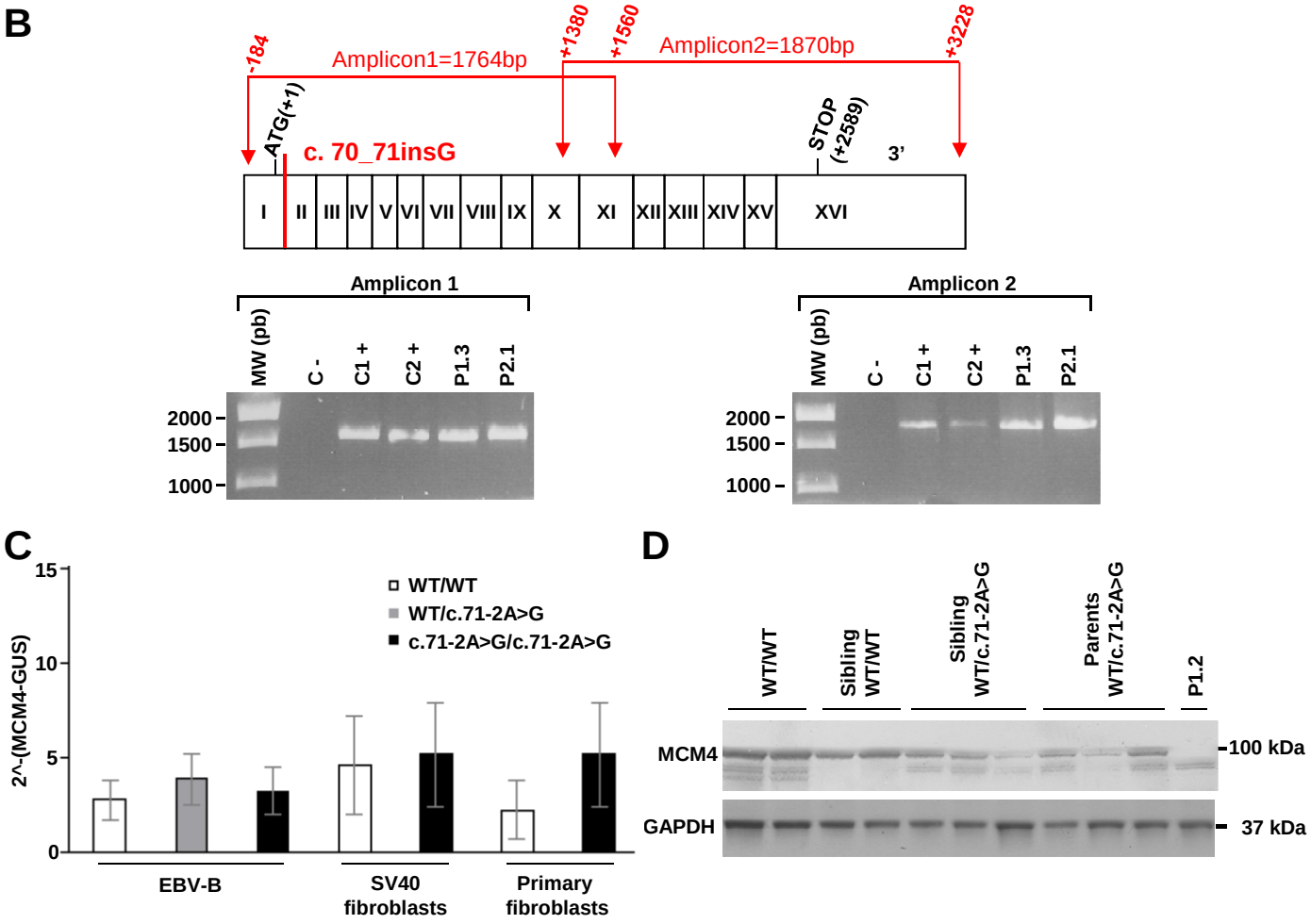

Supplemental Figure 1 (**A**) Table of all variants (other than the causal *MCM4* variant) identified in the coding region, splicing site and the 5' and 3'UTRs of all coding genes and one miRNA located in the centromeric region of chromosome 8. (**B**) Amplification of the *MCM4* cDNA as two fragments. Schematic diagram of the *MCM4* cDNA, showing the binding sites of the primers and the size of the amplification products. Amplification of the *MCM4* cDNA from SV40 fibroblatsts with various primer pairs for controls and patients. (**C**) Relative quantification of *MCM4* mRNA in EBV-B cells from P1.2, family members (n=7, 2 WT/WT, 5 WT/c.71-2A>G) and controls (n=2) and SV40-fibroblasts and primary fibroblasts from P1.3, P2.1 and controls (n=2). We used only probes specific for *MCM4* mRNA. GUS was used as endogenous gene for comparison. The ratio of *MCM4* to GUS mRNA levels is shown. Error bars indicate the standard deviation. (**D**) MCM4 was detected with a polyclonal antibody, at a size of 100 kDa, in total extracts of EBV-B cells from P1.2, WT/WT family members (n=2), WT/c.71-2A>G family members (n=6) and controls (n=2). An antibody against GAPDH was used as a protein loading control.

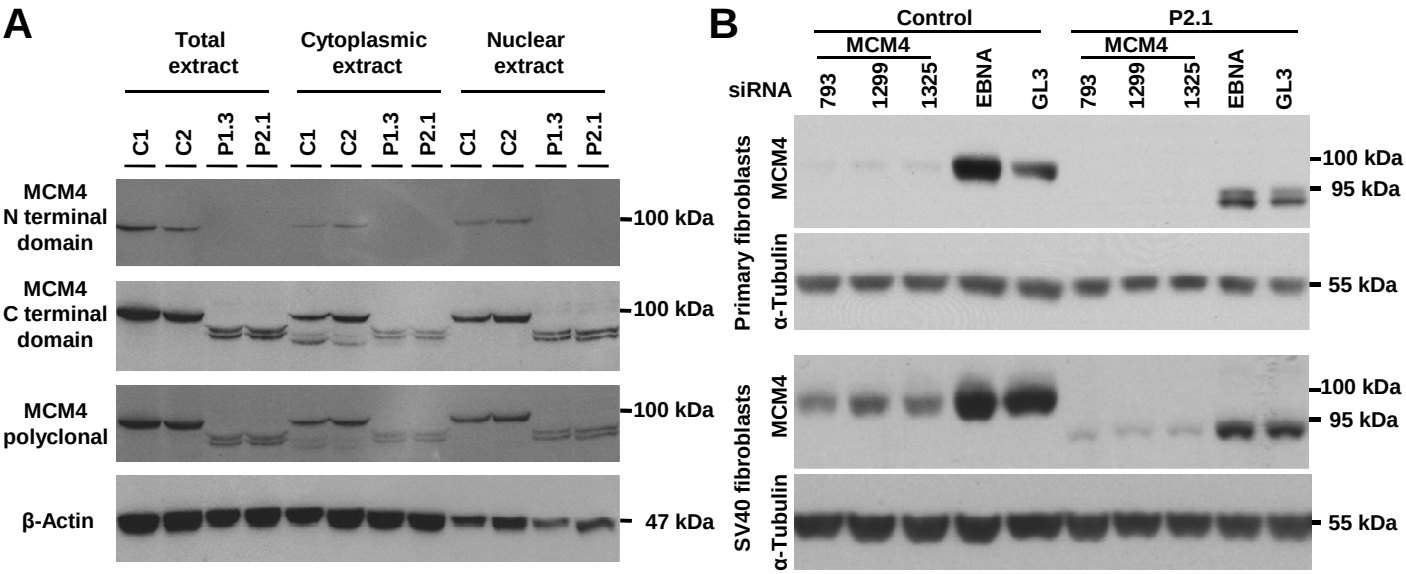

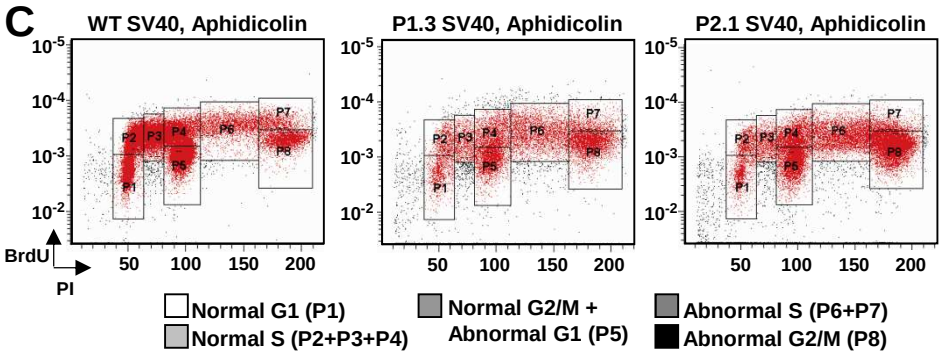

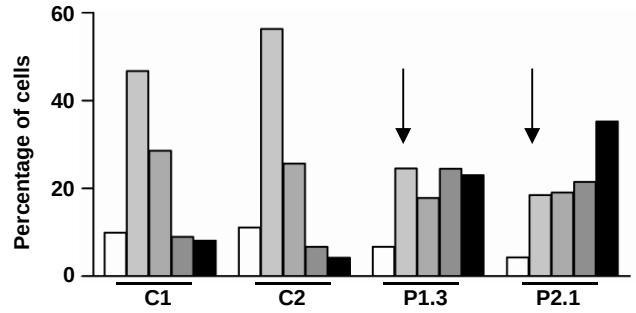

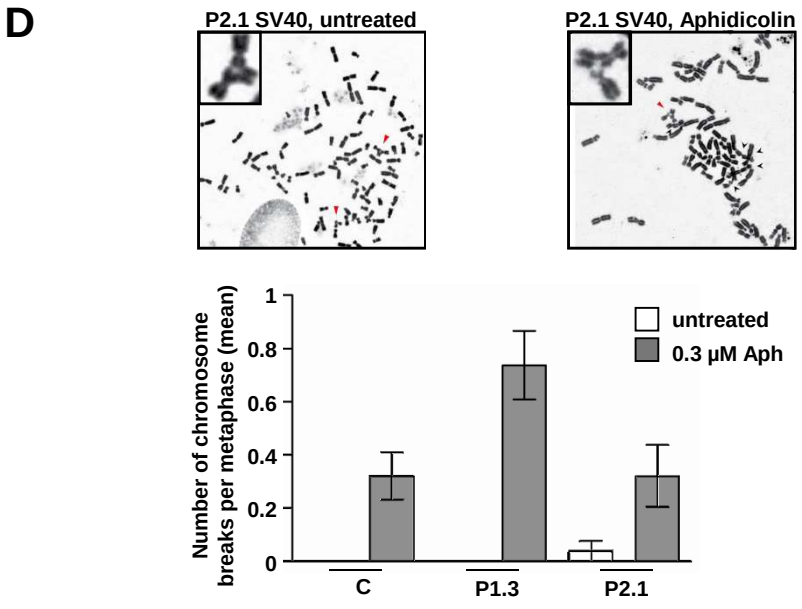

Supplemental Figure 2 (**A**) MCM4 protein production in SV40-fibroblasts from controls, P1.3 and P2.1 was assessed by western blotting with a polyclonal antibody against either the N-terminal domain or the C-terminal domain of MCM4 and a polyclonal antibody against the first 300 amino acids of the MCM4 protein. β-actin antibody was used as a protein loading control. (**B**) MCM4 protein levels after transient transfection with 3 different siRNAs against MCM4 in primary and SV40-fibroblasts from controls and P1.3 assessed by western blotting. Transient transfection with the control siRNAs (EBNA and GL3) was used as a negative control. Total protein extracts from controls and P1.3 primary and SV40-fibroblasts were used as a positive control for the antibody. α-Tubulin antibody was used as a loading control. (**C**) Cell cycle of SV40-fibroblasts from controls and patients after treatment with 0.3 μM Aph. Representative flow cytometry plots. Control (left), P1.3 (middle) and P2.1 (right) after Aph treatment. P1 corresponds to normal G1 phase, P2+P3+P4 correspond to normal S phase, P5 corresponds to normal G2 phase plus abormal G1 or failed mitosis, P6+P7 correspond to re-replication S phase and P8 corresponds to 8C DNA content. The patients' SV40-fibroblasts had a lower proportion of BrdU-positive cells at S phase than the control cells (**D**) Representative spreads of chromosome breaks induced in the presence or absence of APH. A P2.1 metaphase with some aberrations indicated by arrows (left) and a P2.1 metaphase with aphidicolin-induced breaks indicated by arrows (right). The number of chromosome breaks (mean) per metaphase in P1.3 and P2.1 primary fibroblasts was not significantly different from that in control primary fibroblasts. Error bars indicate SEM.

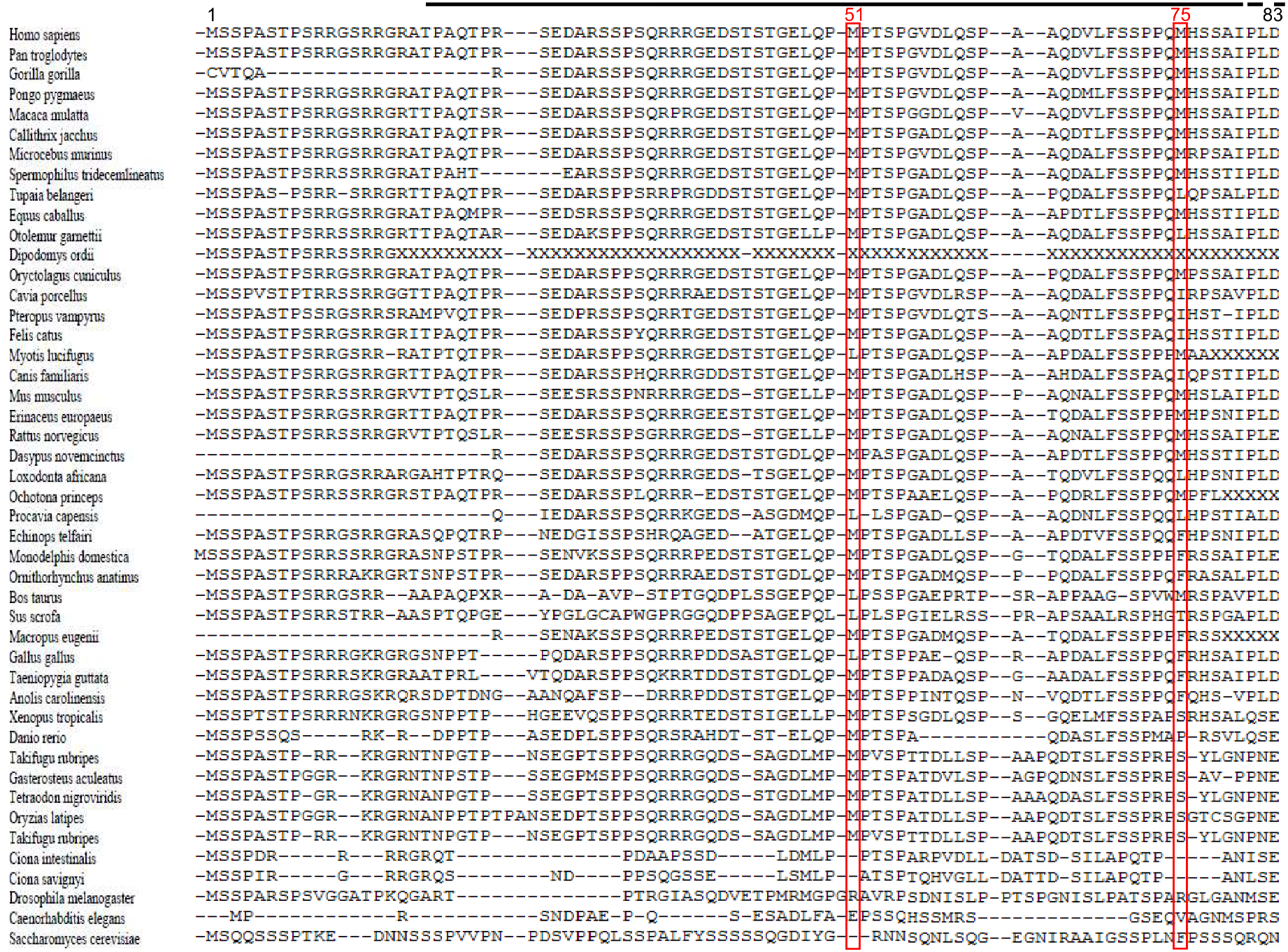

Supplemental Figure 3 The N-terminal domain of the MCM4 protein in humans and the corresponding region in 45 other eukaryotic species. Conservation of the first 83 amino acids of the MCM4 protein, with the position of the three ATG codons in frame.

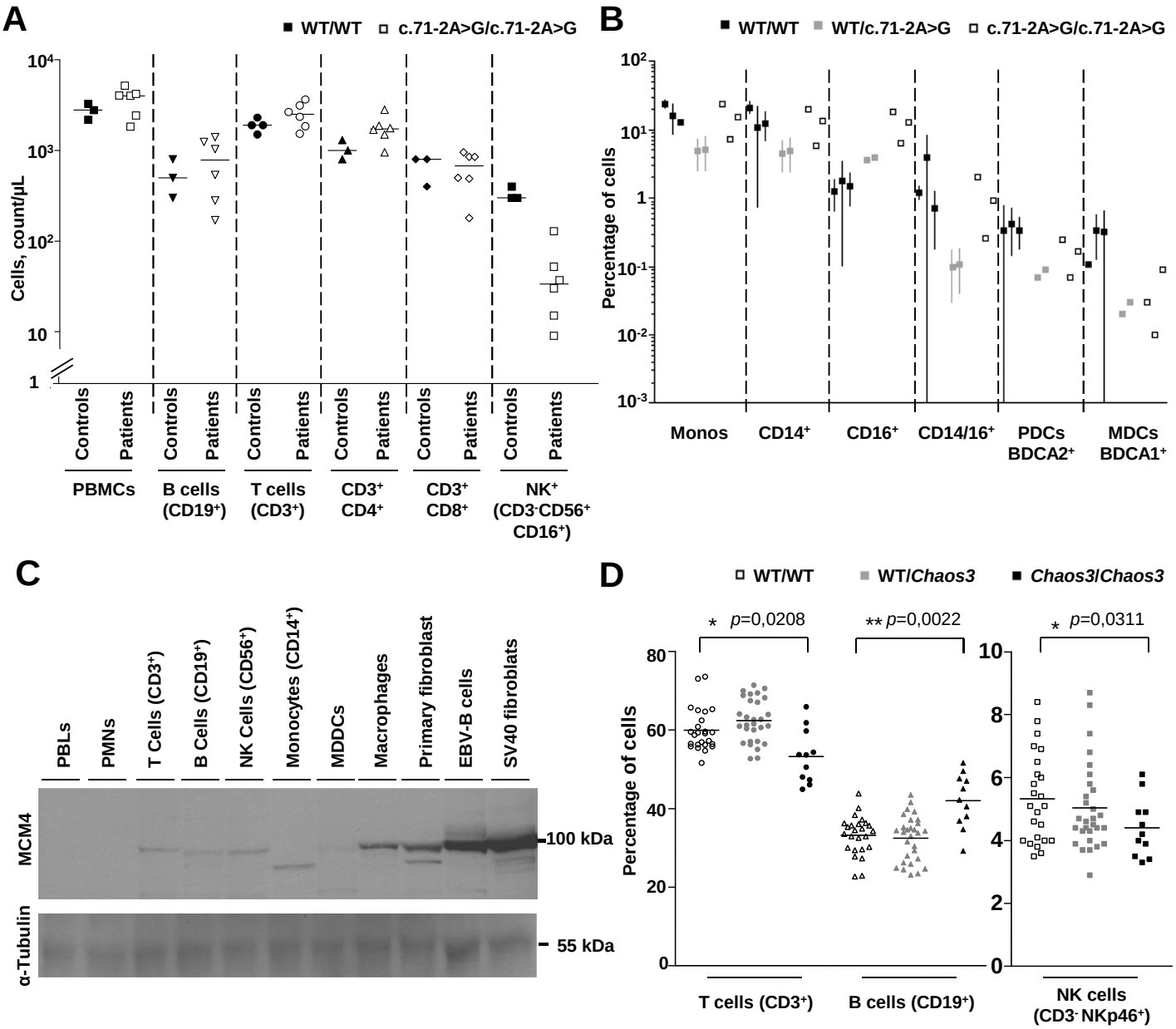

Supplemental Figure 4 Hematopoietic cell phenotypes in humans and mice (**A**) Flow cytometry for lymphocyte subsets: B cells, T cells (CD3+, CD3+CD4+,CD3+CD8+) and NK cells were detected in the peripheral blood of controls and patients (P1.1, P1.2, P1.3 P1.4, P1.5 and P2.1). Horizontal bars represent medians. (**B**) Flow cytometry for monocyte subsets: CD14+, CD16+, CD14/16+ and PDCsBDCA2+ and MDCsBDCA1+ cells were detected in the peripheral blood of controls of various age groups (5 to 10 y, 10 to 15 y and >15 y), heterozygous subjects and homozygous patients (P1.1, P1.2 and P1.3). Error bars for the controls indicate the standard deviation. (**C**) MCM4 was detected with a polyclonal antibody, at a size of 100 kDa, in cell subsets from blood (PBLs, PMNs, T cells, B cells, NK cells, monocytes, MDDCs and macrophages), EBV-B cells, primary and SV40 fibroblast cells from a control individual. An antibody against α-tubulin was used as a loading control. This result is representative of 3 independent experiments). (**D**) NK cell percentage in WT/WT, *Chaos3*/WT, *Chaos3*/*Chaos3* mice. The percentage of NK cells is significantly lower in *Chaos3*/*Chaos3* (n=11) than in WT/WT (n=25) mice (P <0.05 indicated by *, non parametric Wilcoxon test). Horizontal bars indicate the means. The percentage of B cells is significantly higher in *Chaos3*/*Chaos3* (n=11) than in WT/WT (n=25) mice (P <0.005 indicated by **, non parametric Wilcoxon test). A significant difference in the percentage of T cells was observed between WT/WT (n=19) and *Chaos3*/*Chaos3* (n=11) mice (P <0.05 indicated by *, non parametric Wilcoxon test).

A

Cell Subsets	Sibling WT/WT	Sibling WT/c.71-2A>G		P1.1 c.71-2A>G/c.71-2A>G	P1.2 c.71-2A>G/c.71-2A>G	P1.3 c.71-2A>G/c.71-2A>G	Normal range
T-CD3$^+$ (%)	69	73	77	76	76	67	56-84
T-CD4$^+$ (%)	38	47	41	54	34	43	31-52
CD4$^+$CD45RA$^+$ (%)	26	ND[a]	22	66	39	29	20-86
CD4$^+$CD45RO$^+$ (%)	74	ND	87	34	64	71	29-63
T-CD8$^+$ (%)	26	23	26	21	26	22	18-35
CD8$^+$CD45RA$^+$ (%)	65	47	78	68	29	34	40-80
CD8$^+$CD45RO$^+$ (%)	39	49	75	33	71	73	12-43
B-CD19$^+$ (%)	14	14	16	23	20	30	6-23
CD19$^+$ CD27$^+$(%)	11	16	21	4	10	5	>10

[a] Not Done

B

Stimulus 3 days culture	Sibling WT/WT	Sibling WT/c.71-2A>G		P1.1 c.71-2A>G/c.71-2A>G	P1.2 c.71-2A>G/c.71-2A>G	P1.3 c.71-2A>G/c.71-2A>G	Normal range
Medium	**0.1**	**0.1**	**0.1**	**0.25**	**0.15**	**0.3**	
PHA	**179**	**78.5**	**98**	**100**	**43.5**	**97**	**>50**

* Cpm/10*3

C

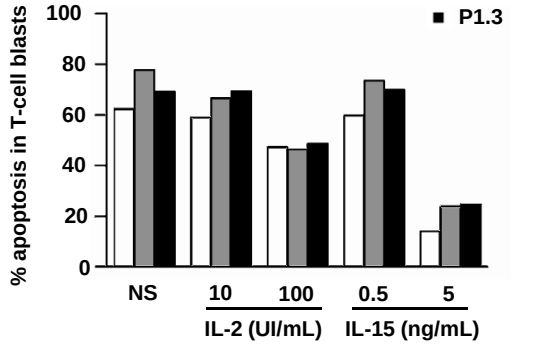

D

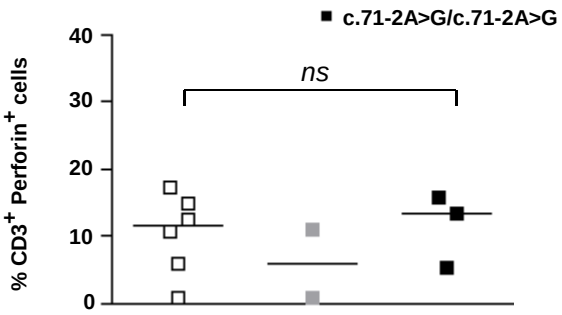

Supplemental Figure 5 T-cell phenotypes and stimulation responses (**A**) Percentage of different T- and B-cell subsets in whole-blood samples from healthy siblings either homozygous WT or heterozygous, and patients. (**B**) Proliferation of PBMCs determined by thymidine incorporation from healthy homozygous WT or heterozygous siblings and patients were not stimulated (medium) or were stimulated with PHA (2.5 mg/ml) over 3 days. (**C**) Apoptosis of PHA-activated T-cell blasts from a control, P1.2 and P1.3 was assessed by determining propidium iodide staining in the presence or absence of stimulation with various doses of IL-2 or IL-15 over 3 days. (**D**) Flow cytometry counts of CD3+Perforin+ T cells for controls (n=6), heterozygous siblings (n=2) and patients (P1.1, P1.2 and P1.3). Horizontal bars indicate medians. A non significant difference (*P*>0.05) is indicated by “ns”.

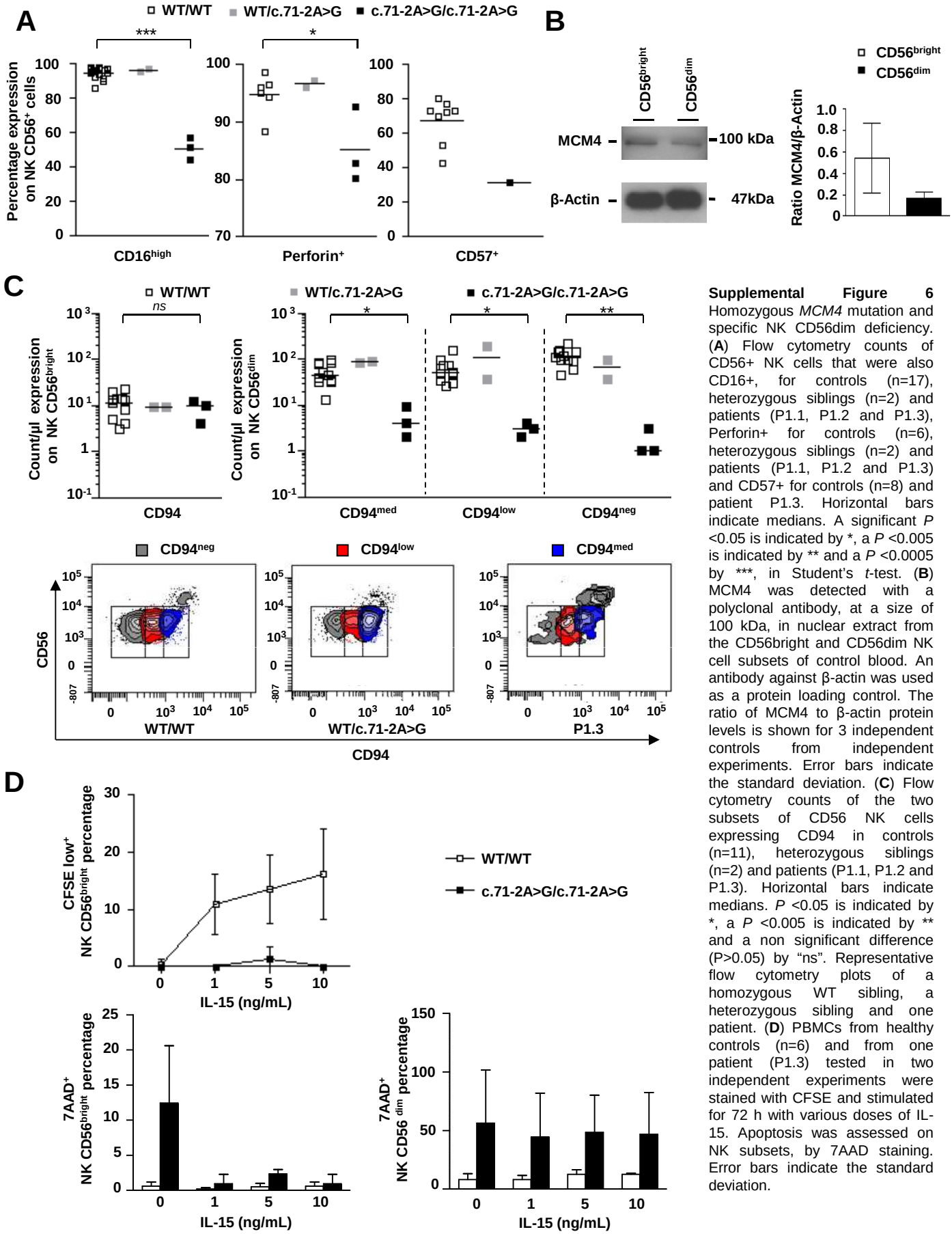

Supplemental Figure 6 Homozygous *MCM4* mutation and specific NK CD56dim deficiency. (**A**) Flow cytometry counts of CD56+ NK cells that were also CD16+, for controls (n=17), heterozygous siblings (n=2) and patients (P1.1, P1.2 and P1.3), Perforin+ for controls (n=6), heterozygous siblings (n=2) and patients (P1.1, P1.2 and P1.3) and CD57+ for controls (n=8) and patient P1.3. Horizontal bars indicate medians. A significant *P* <0.05 is indicated by *, a *P* <0.005 is indicated by ** and a *P* <0.0005 by ***, in Student's *t*-test. (**B**) MCM4 was detected with a polyclonal antibody, at a size of 100 kDa, in nuclear extract from the CD56bright and CD56dim NK cell subsets of control blood. An antibody against β-actin was used as a protein loading control. The ratio of MCM4 to β-actin protein levels is shown for 3 independent controls from independent experiments. Error bars indicate the standard deviation. (**C**) Flow cytometry counts of the two subsets of CD56 NK cells expressing CD94 in controls (n=11), heterozygous siblings (n=2) and patients (P1.1, P1.2 and P1.3). Horizontal bars indicate medians. *P* <0.05 is indicated by *, a *P* <0.005 is indicated by ** and a non significant difference (P>0.05) by "ns". Representative flow cytometry plots of a homozygous WT sibling, a heterozygous sibling and one patient. (**D**) PBMCs from healthy controls (n=6) and from one patient (P1.3) tested in two independent experiments were stained with CFSE and stimulated for 72 h with various doses of IL-15. Apoptosis was assessed on NK subsets, by 7AAD staining. Error bars indicate the standard deviation.